GEOLOGIJA 57/2, 183-192, Ljubljana 2014

doi:10.5474/geologija.2014.016

Electrical resistivity tomography investigations along the planned dykes of the HPP Brežice water accumulation basin

Raziskave z električno upornostno tomografijo vzdolž trase nasipov akumulacijskega bazena HE Brežice

Gregor RAJH[1], Marjeta CAR[2] & Andrej GOSAR[3,4]

[1]Usnjarska cesta 23, SI–1241 Kamnik; e-mail: rajhgregor@gmail.com
[2]Geoinženiring d.o.o., Dimičeva ulica 14, SI–1000 Ljubljana; e-mail: marjeta.car@geo-inz.si
[3]ARSO, Urad za seizmologijo in geologijo, Vojkova 1b, SI–1000 Ljubljana, e-mail: andrej.gosar@gov.si
[4]Naravoslovnotehniška fakulteta, Aškerčeva 12, SI-1000 Ljubljana

Prejeto / Received 3. 11. 2014; Sprejeto / Accepted 15. 12. 2014

Key words: geophysics, HPP Brežice, Krško-Brežice field, electrical resistivity tomography, sediments, jet grouting, electrical resistivity, geoelectrical model
Ključne besede: geofizika, HE Brežice, Krško-Brežiško polje, električna upornostna tomografija, sedimenti, jet grouting, električna upornost, geoelektrični model

Abstract

Geophysical investigations were conducted using electrical resistivity tomography (ERT) along planned dykes of the HPP Brežice water accumulation basin. The ERT profile is 7.3 km long and is located on the right riverbank of the Sava River on the Krško-Brežice field (E Slovenia). A purpose of the investigations was to determine a boundary between semipermeable Miocene and permeable Plio-Quaternary (Pl-Q) and Quaternary (Q) sediments for the proper design of the jet grouting sealing curtain, which will prevent lateral outflow of water from the accumulation basin. In this paper we present processing of the section between 5100 and 6100 m of the profile line. In this section the measurement template was set to 25 depth levels, because a significant increase in a thickness of the Pl-Q sediments was expected. Modelling of the measured apparent electrical resistivity data was carried out with RES2DINV and RESIX 2DI inversion software. Different inversion parameters were used to create 15 geoelectrical models for each program, which were then compared and evaluated based on borehole data and on previous geological investigations of the area. With the final geoelectrical models it was possible to successfully determine areas of three expected stratigraphic members and limit an electrical resistivity range for each one of them. The boundary is well defined between Q and Pl-Q and also between Q and Miocene sediments with sharp contrast in electrical resistivity between them. A boundary between Pl-Q and Miocene sediments was not that obvious, but it was possible to determine its shape by the use of different inversion parameters. We propose a simplified geological cross section based on the interpreted geoelectrical models and borehole data.

Izvleček

Geofizikalne raziskave z metodo električne upornostne tomografije so bile izvedene po 7,3 km dolgemu profilu, ki poteka vzdolž načrtovanih nasipov za HE Brežice na desnem bregu Save na Krško-Brežiškem polju. Namen raziskav je bil določiti mejo med polprepustnimi miocenskimi ter prepustnimi pliokvartarnimi (Pl-Q) in kvartarnimi (Q) sedimenti za načrtovanje t.i. jet grouting tesnilne zavese, ki bo preprečevala lateralni odtok vode iz akumulacijskega bazena. V članku predstavljamo obdelavo odseka med 5100 in 6100 m profila na katerem smo pričakovali začetek pojavljanja večje debeline Pl-Q sedimentov, zato smo meritve izvedli na 25 globinskih nivojih. Modeliranje izmerjenih podatkov navidezne električne upornosti je potekalo s programoma RES2DINV in RESIX 2DI z uporabo različnih parametrov pri izdelavi modelov. Te smo med seboj primerjali in vrednotili na podlagi preteklih geoloških raziskav območja in podatkov vrtin. Z vsakim programom smo izdelali 15 različnih modelov. S končnimi modeli smo lahko uspešno opredelili območja pojavljanja treh pričakovanih stratigrafskih členov in za vsakega podali razpon modeliranih električnih upornosti. Na modelih je dobro viden potek meje med Q in Pl-Q ter med Q in miocenskimi sedimenti z velikim medsebojnim kontrastom v električni upornosti. Nekoliko slabše je definirana meja med Pl-Q in miocenskimi sedimenti, vendar je bilo z uporabo različnih postopkov modeliranja tudi mogoče opredeliti njeno obliko. Na podlagi izdelanih modelov in podatkov vrtin smo za obdelan odsek podali poenostavljen geološki profil, na katerem so predstavljene glavne geoelektrično ugotovljene meje med stratigrafskimi členi.

Introduction

Electrical resistivity tomography (ERT) investigations were conducted along planned dykes of the HPP Brežice water accumulation basin (Fig. 1a). The profile is 7.3 km long and located on the right riverbank of the Sava River. Investigations on the left riverbank were conducted by another contractor and were not yet ready for comparison with our results. A purpose of the investigations was to determine a boundary between semipermeable Miocene and permeable Plio-Quaternary (Pl-Q) and

Quaternary (Q) sediments in order to properly design a jet grouting sealing curtain, which will prevent lateral outflow of water from the accumulation basin. Based on previous investigations of the area (e.g. Lapajne, 1975), gradual thickening of the Pl-Q sediments was expected in a section between 5100 and 6100 m of the profile line. Geoelectrical differentiation of Pl-Q sediments presents an interesting challenge for a geophysicist, which is why we decided to present this section in the paper.

Electrical resistivity tomography

ERT investigations combine 1D techniques of vertical electrical sounding and resistivity mapping. Investigations are conducted along a continuous profile line for different depth levels, defined by a different spacing between electrodes. In this way we are able to observe lateral and vertical (2D) variations in electrical resistivity (Car, 1995; Møller et al., 2006).

Before data acquisition a certain number of electrodes is laid along a profile line and connected with a multicore cable to an electrode switcher, which defines a number and a role (current/potential) of each electrode. The whole process is automatically controlled by a central processing unit (CPU) with an electrical resistivity meter. Parameters required to successfully conduct the measurements for chosen depth levels, electrode array and spacing are inserted into the CPU or a laptop computer. For each measurement, an electrical impulse is transmitted into the ground through the chosen pair of current electrodes and as a result potential drop is measured on

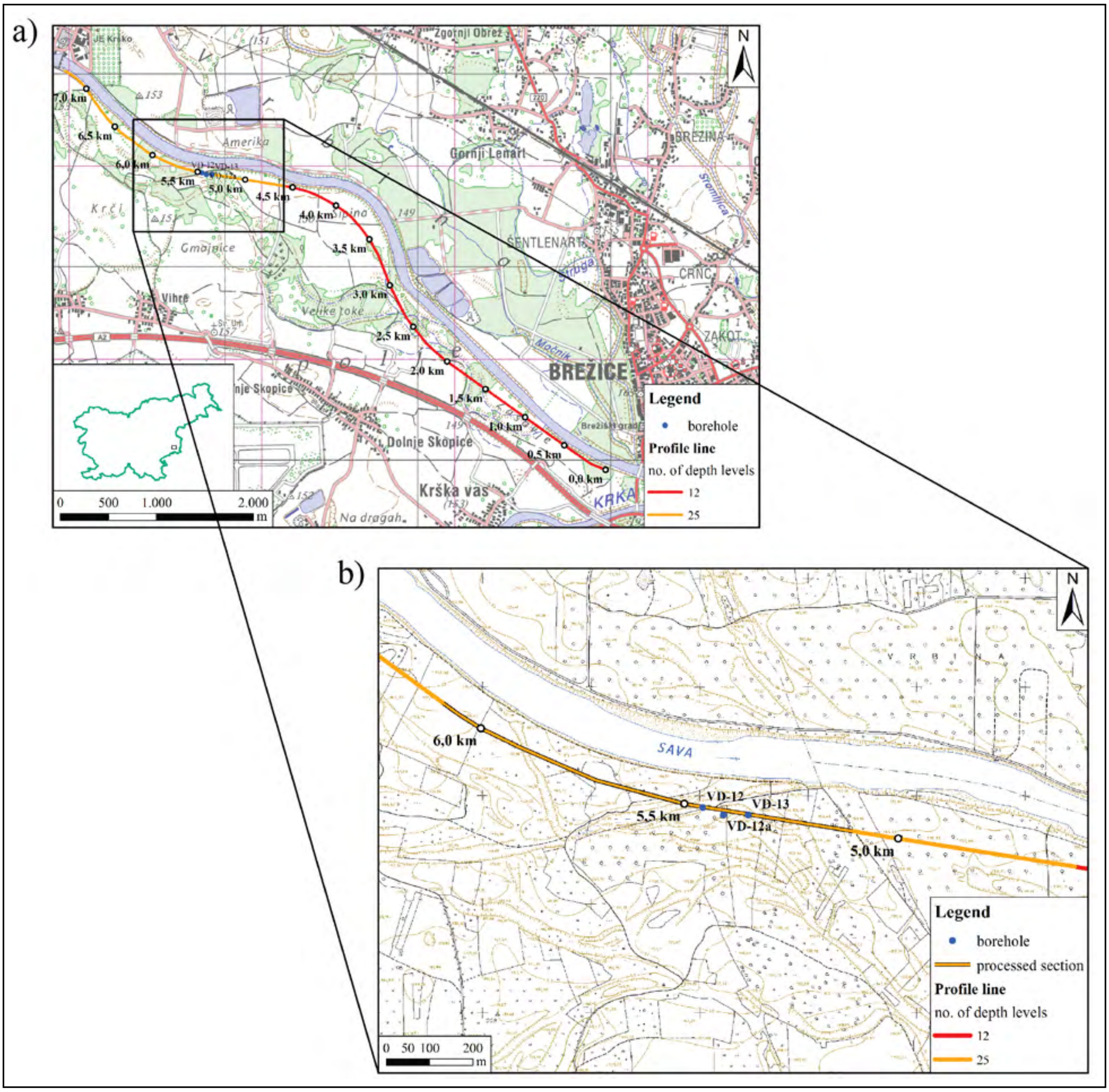

Fig. 1. a) Location of geoelectrical profile and b) situation of processed section with borehole locations.

Sl. 1. a) Položaj geoelektričnega profila in b) podrobnejša situacija obdelanega odseka in vrtin.

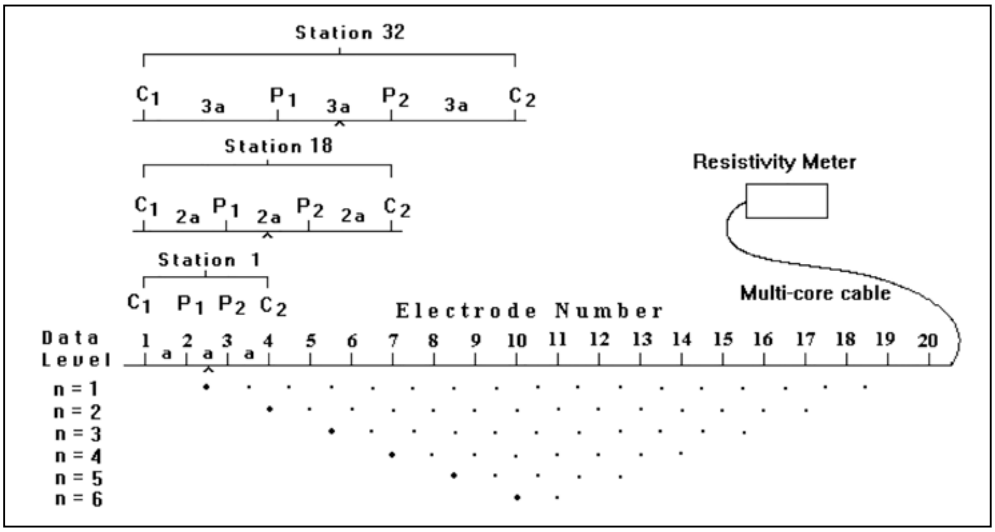

Fig. 2. Electrical resistivity tomography data acquisition process for Wenner electrode array (Loke, 2014).

Sl. 2. Shematski prikaz globinskih nivojev merskih točk psevdosekcije za Wennerjevo elektrodno razvrstitev (Loke, 2014).

the chosen pair of potential electrodes at a time. The whole system is powered by a battery or a power generator. Measurements are conducted for all pre-defined electrode combinations on different depth levels. Each depth level is defined by the spacing between the electrodes. A process of data acquisition is schematically shown on Figure 2. Measured apparent resistivity values are shown on a resistivity pseudosection, which is of a trapezoidal shape (Car, 1995; Møller et al., 2006; Loke, 2014).

For an interpretation of data acquired by ERT, different inversion programs are used. A modelling procedure includes a 2D inversion of measured data by using an iterative least squares method, for which adjustments are made based on a model response, calculated by a finite element method. Each consecutive model is iteratively adjusted until fit between measured and calculated data (RMS error) converges at a certain value. A RMS error can be a good quantitative indicator for a model quality, but not necessary for actual geological conditions in subsurface. If possible, every model should be evaluated based on existing geological investigations of an area and borehole data (Fehdi et al., 2011; Loke, 2014).

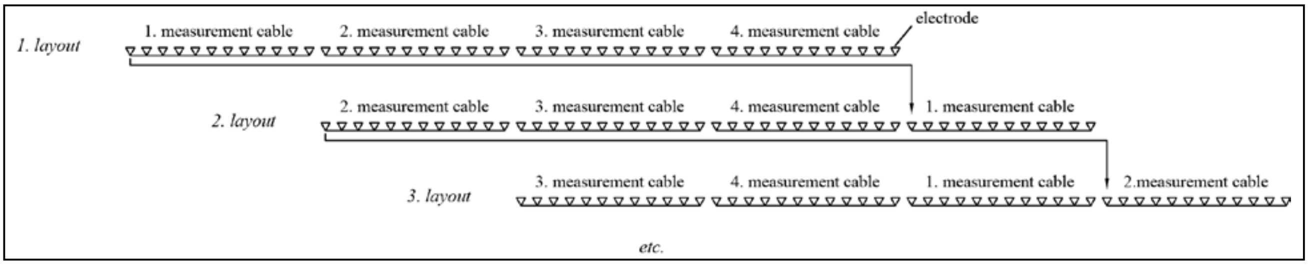

Fig. 3 Cables manoeuvring by using roll-along technique.

Sl. 3. Shematski prikaz premeščanja merskih kablov s tehniko „roll-along“.

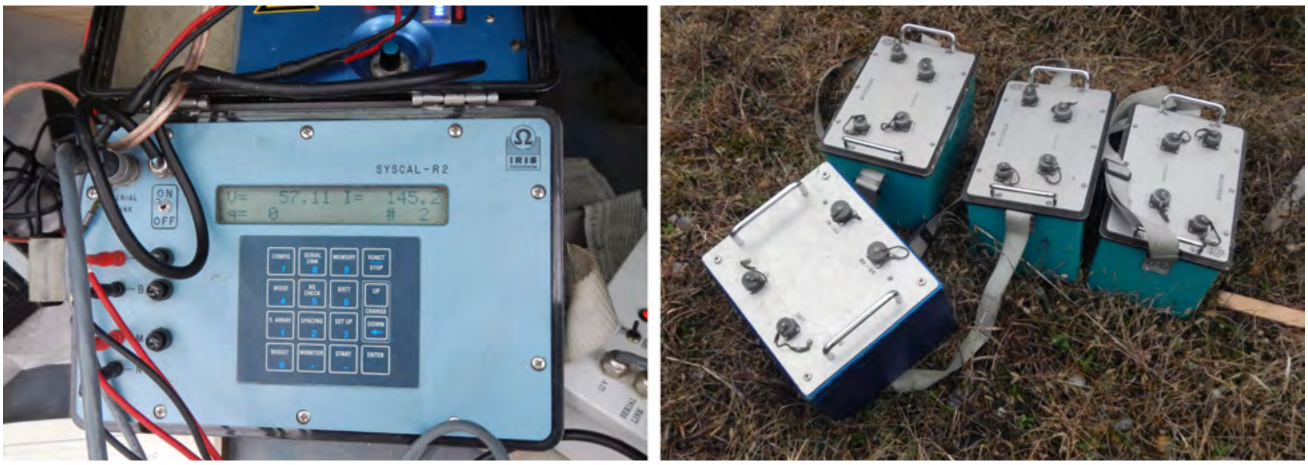

Fig. 4. Syscal R2 central processing unit (left) and electrode switchers (right).

Sl. 4. Centralna procesna enota Syscal R2 (levo) in elektrodni preklopniki (desno).

Measurements and modelling

ERT measurements were conducted in the December 2013 during dry and stable weather conditions and in relatively moist ground. On the selected section we used the Wenner electrode array for 25 depth levels. Multicore measurement cables with 12 electrode take-outs on every 5 m were used. The electrode line of eight measurement cables layout was horizontally extended using a roll-along technique, where a first cable is disconnected and placed to the end of a profile line, when all predefined electrode combinations on its length are completed (Fig. 3). This process of cable replacement is repeated on all consecutive cables, until a needed profile length is achieved. The technique was introduced to ERT by van Overmeeren and Ritsema (1988). We used the Syscal R2 CPU and electrode switchers from Iris instruments (Fig. 4).

Modelling of measured apparent electrical resistivity data was carried out using RES2DINV v. 3.59 (Geotomo Software, Loke, 2010) and RESIX 2DI v. 4.17 (Interprex Limited, Stoyer & Butler, 2001) computer inversion programs. Both programs allow manual determination of different inversion parameters and values.

Table 1. Data from boreholes VD12, VD12a and VD13.

Tabela 1. Podatki vrtin VD12, VD12a and VD13.

Borehole (position on the profile)	boundary silt/Q gravel	boundary Q gravel/ Pl-Q gravel	boundary Pl-Q gravel/ Miocene marl
VD13 (5380 m)	1 m	10,1 m	11 m
VD12a (5430 m)	2,2 m	11,2 m	17,9 m
VD12 (5600 m)	1,3 m	11 m	42,4 m

Table 2. Overview of chosen parameters and values for models 1, 2 and 3.

Tabela 2. Prikaz izbranih parametrov in vrednosti za modele 1, 2 in 3.

Parameter	Choice/value$^{(model\ number)}$
density of finite element mesh	normal$^{(1,2,3)}$
number of nodes per unit electrode spacing	2$^{(1,2,3)}$
width of model blocks	same as electrode spacing$^{(1,2,3)}$
factor to increase cell thickness with depth	1,10$^{(1,2,3)}$
maximum number of iterations	5$^{(1,2,3)}$
smoothing of model resistivity	YES$^{(1,2,3)}$
use combined inversion method	YES$^{(3)}$/NO$^{(1,2)}$
recalculate Jacobian matrix	first two iterations$^{(1,2,3)}$
Jacobian matrix calculation	Gauss-Newton for first two iterations, then quasi-Newton$^{(1,2,3)}$
use robust optimization method	YES$^{(2)}$/NO$^{(1,3)}$
damping factor (initial/ minimum/first layer)	0,3/0,03/5$^{(2,3)}$, 0,3/0,1/0$^{(1)}$
change of damping factor with depth	automatic calculation$^{(1)}$/fixed value (1,1)$^{(2,3)}$
type of initial model	homogeneous half-space$^{(1,2,3)}$
vertical/horizontal flatness ratio	1$^{(2,3)}$, 0,7$^{(1)}$

Table 3. Overview of chosen parameters and values for models 4, 5 and 6.

Tabela 3. Prikaz izbranih parametrov in vrednosti za modele 4, 5 in 6.

Parameter	Choice/value$^{(model\ number)}$
horizontal element width	1 m$^{(4,5,6)}$
vertical element height within topography	0,25 m$^{(4,5,6)}$
vertical element height below topography (number of elements)	1 m (5)$^{(4,5,6)}$
deep pad vertical element height (factor to increase with depth)	1 m (1,2)$^{(4,5,6)}$
maximum number of iterations	5$^{(4,5,6)}$
influence sphere	10 electrodes$^{(4,5,6)}$
inversion method (regularization)	ridge regression$^{(4)}$, Occam's$^{(5,6)}$
Jacobian matrix calculation for first iteration	approximate$^{(4,5,6)}$
Jacobian matrix calculation for other iterations	quasi-Newton$^{(4,5,6)}$
calculation of damping factor	automatic, fast$^{(4,5,6)}$
damping factor (minimum/ maximum)	0,0004/0,05$^{(4,5,6)}$
type of initial model	homogenous half-space$^{(4,5,6)}$
vertical/horizontal flatness ratio	1$^{(4,5)}$, 0,7$^{(6)}$

Available data

For the investigated area, borehole data and data from previous geophysical investigations were available. Data from three boreholes (Fig. 1b) are presented in Table 1 and on Figure 5, where distinctive thickening of Pl-Q silty and sandy gravel towards the NW is visible. Based on previous geophysical investigations conducted on the Krško-Brežice field (Lapajne, 1975; Car & Stopar, 2008), we limited electrical resistivity ranges of modelled values for each geoelectrical layer, representing different stratigraphic members (Fig. 6). A range of the expected electrical resistivity for Q gravel and sandy gravel was ascertained to 300-5000 Ωm. Lower values, i.e. 100-300 Ωm, correspond to Pl-Q silty and sandy gravel and 10-100 Ωm to Miocene marl, sandy marl and sandy silt sediments.

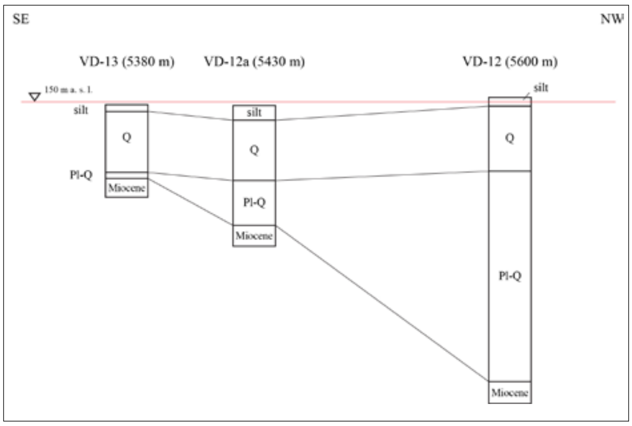

Fig. 5. Schematic view of borehole data.

Sl. 5. Shematski prikaz podatkov vrtin.

Results

Results from the ERT measurements were analysed using pseudosection, model response and model as on Figure 7. In the modelling process, different inversion parameters were used to create a total of 15 geoelectrical models for each program. In this paper we show three selected geoelectrical models for each program (Fig. 9 and 10), which best represent the difference between the chosen parameters (Tables 2 and 3).

RES2DINV

With RES2DINV we created models using the identical model grid (Fig. 8). The models created with this program are shown on Figure 9 and corresponding parameters are presented in Table 2. We fixed a logarithmic colour scale for an easier comparison between the models. On all presented models we see three layers with different electrical resistivity values. The shallowest layer with the highest values (360-1100 Ωm) is approximately 10 m thick and enclose two layers with lower electrical resistivities. The SE part of the models on Figure 9 is characterised by electrical resistivities 15-70 Ωm. On the other hand, resistivity values between 80 and 220 Ωm are observed in the NW part of the models. At both ends, the thickness of two electrical units exceeds 50 m. However, in the central part of the profile the thickness of the unit with 80-220 Ωm increases towards the NW and it seems that the lower resistivity unit deepens under the higher resistive one.

From the comparison of presented models we see that the use of the robust optimization method gave us model 2 (Fig. 9b) with very low RMS error of 3.5 %. Despite its low error value

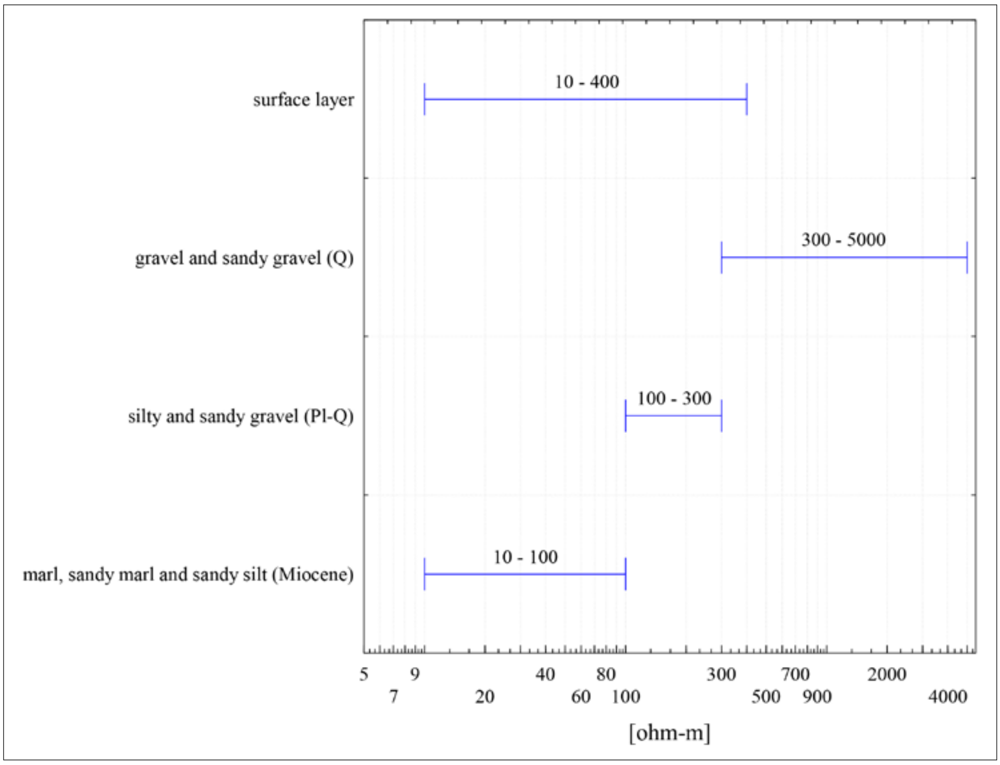

Fig. 6. Modelled electrical resistivity ranges for individual stratigraphic members at Krško-Brežice field (after Lapajne, 1975; Car et al., 2008).

Sl. 6. Modelirani intervali el. upornosti za posamezne stratigrafske člene na Krško-Brežiškem polju (po Lapajne, 1975; Car et al., 2008).

this model is only an approximation of actual subsurface geological conditions, due to the unrealistic resistivity distribution and steep boundaries between different resistivity areas (bodies). Models 1 and 2, on Figures 9a and 9b respectively, show more homogenous bodies, because we used different inversion methods and higher values of damping factors. Lower vertical/horizontal flatness ratio also played a key role, by making oblique boundaries smoother in model 1.

RESIX 2DI

Models created with RESIX 2DI are shown on Figure 10 and used parameters in Table 3. The colour scale was again fixed for all models. Layers of different electrical resistivities appear similarly as with RES2DINV. The one with the highest values (300-6000 Ωm) of electrical resistivity and a thickness of 10-15 m, extends over the entire upper part of the models. Underneath are two thicker layers. One in the SE part of the models with electrical resistivity values up to 100 Ωm and another one in the NW part with the values of 100-300 Ωm. The oblique boundary between them is not that well defined as it was on models created with RES2DINV, but we are still able to approximate it by the comparison of presented models.

Presented RESIX 2DI models were created by choosing different inversion methods and lower vertical/horizontal flatness ratio. The ridge regression inversion method, used in modelling of model 4 (Fig. 10a), gave the most homogenous body in the SE part of the profile. In this area the Occam's inversion method produced model 5 (Fig. 10b) with lense shaped bodies, which are elongated in the NW direction. These bodies were partially smoothed out with the use of lower vertical/horizontal flatness ratio to create model 6 (Fig. 10c).

Conclusions

Selected geoelectrical models were compared and evaluated considering existing geological investigations of the area and borehole data. With two chosen geoelectrical models (Fig. 11) it was

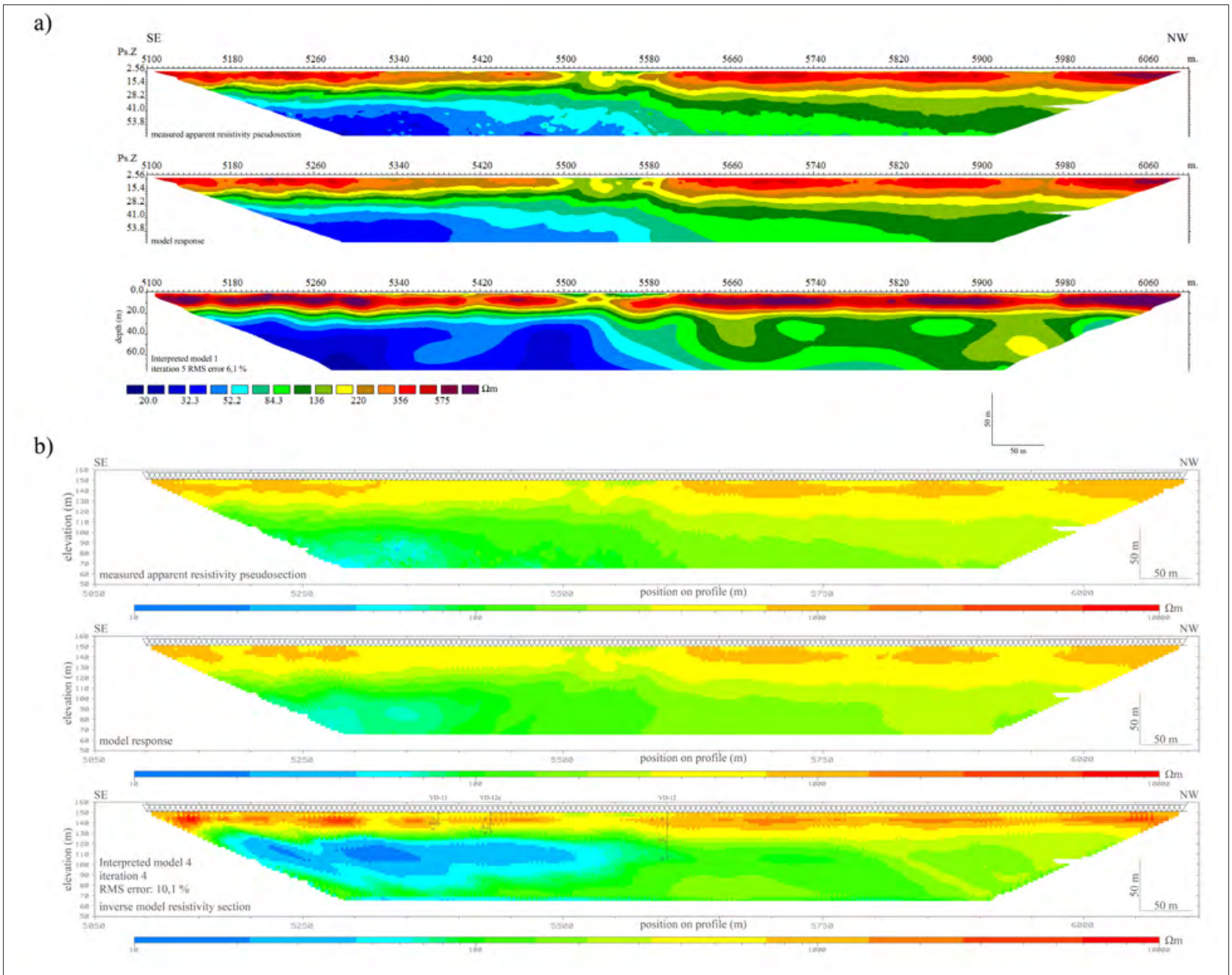

Fig. 7. Modelling result shown with pseudosection, model response and model for a) RES2DINV and b) RESIX 2DI.
Sl. 7. Rezultat modeliranja prikazan z upornostno psevdosekcijo, odzivom modela in modelom za a) RES2DINV and b) RESIX 2DI.

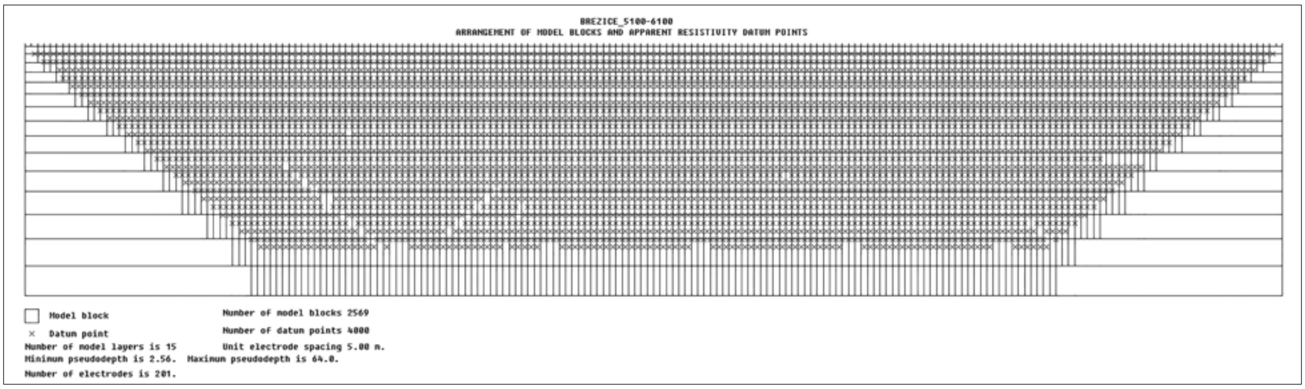

Fig. 8. Distribution of model grid with measured data points for presented models.
Sl. 8. Razporeditev mreže celic s prikazanimi merskimi točkami za predstavljene modele.

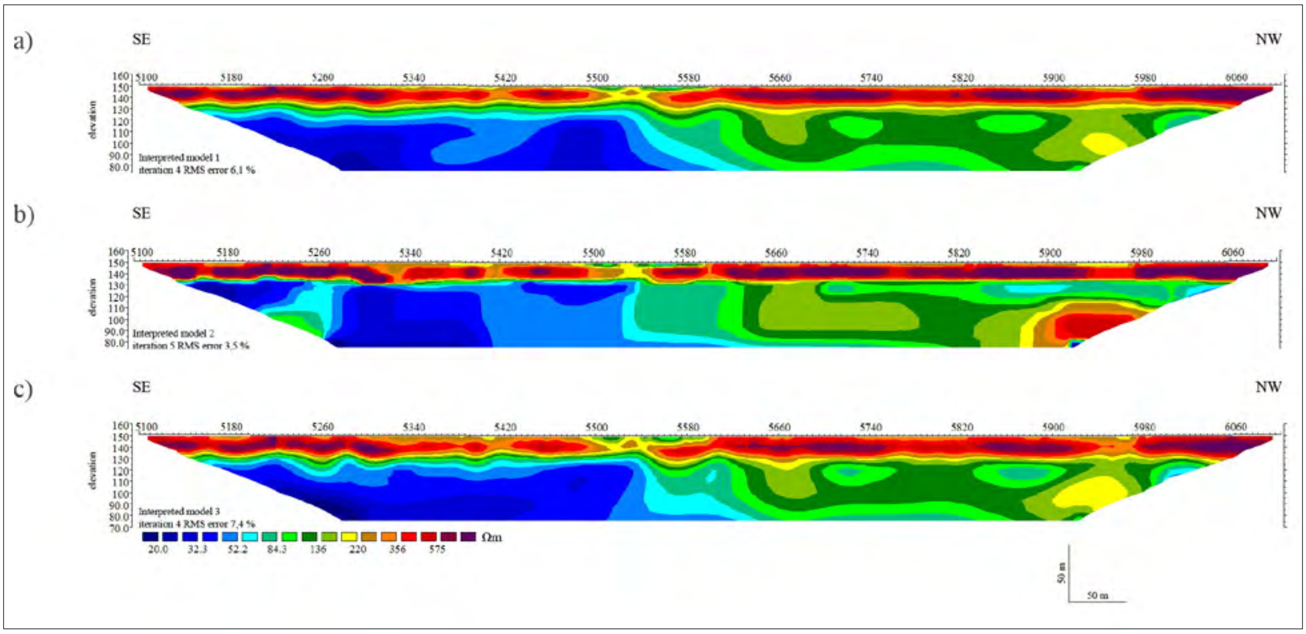

Fig. 9. Models created with RES2DINV: a) Model 1, b) Model 2 and c) Model 3.
Sl. 9. Modeli izdelani s programom RES2DINV: a) model 1, b) model 2 in c) model 3.

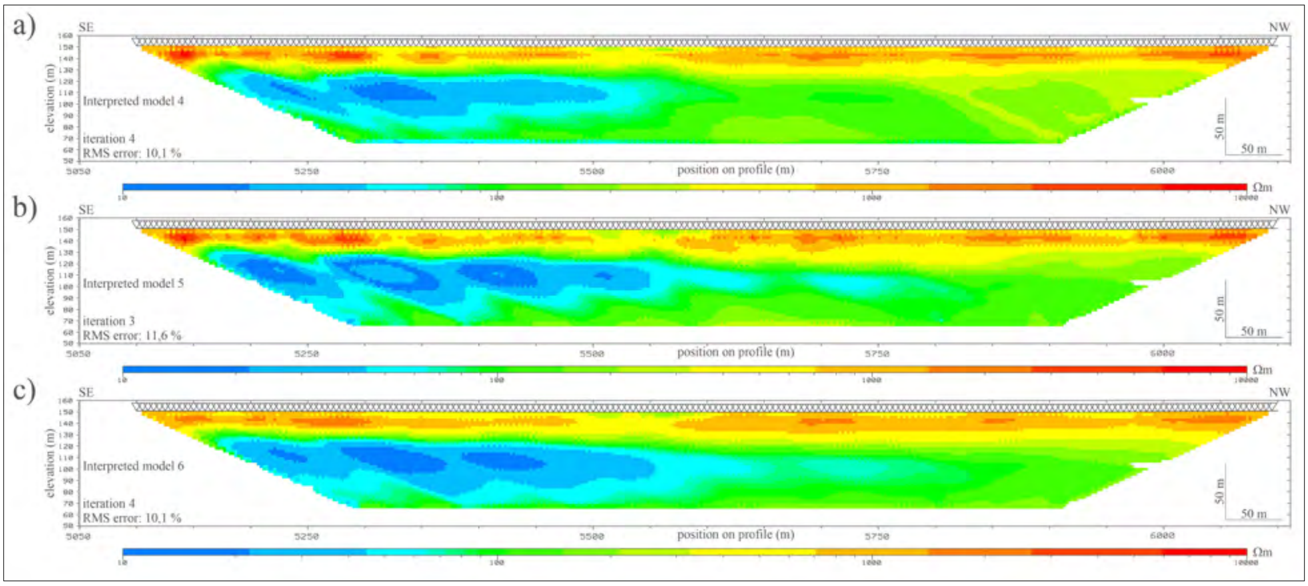

Fig. 10. Models created with RESIX 2DI: a) Model 4, b) Model 5 and c) Model 6.
Sl. 10. Modeli izdelani s programom RESIX 2DI: a) model 4, b) model 5 in c) model 6.

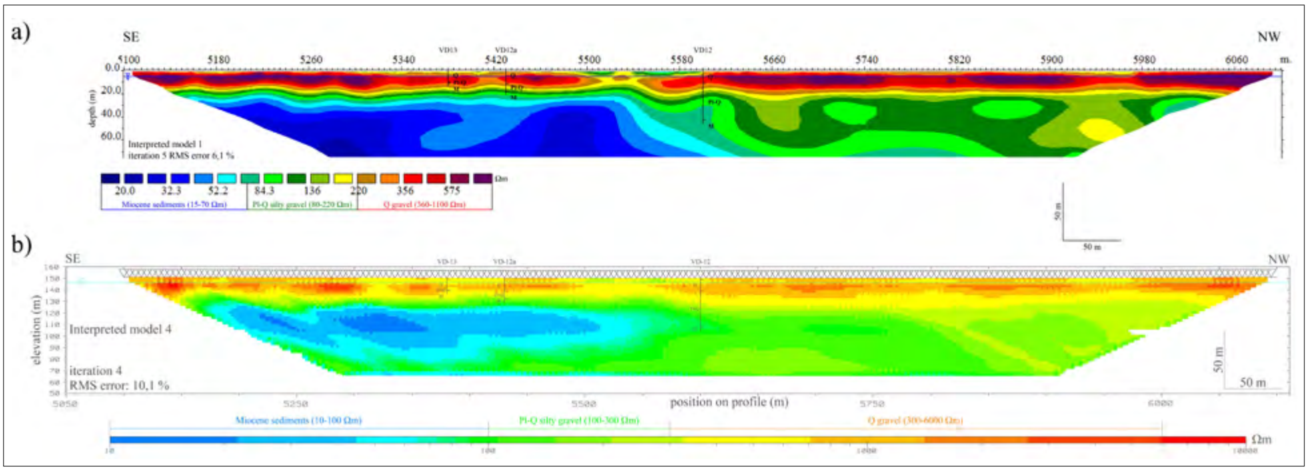

Fig. 11. Final two models with electrical resistivity scales and borehole data for each program: a) RES2DINV and b) RESIX 2DI.
Sl. 11. Izbrana modela za vsakega izmed programov s podanima skalama električne upornosti: a) RES2DINV in b) RESIX 2DI.

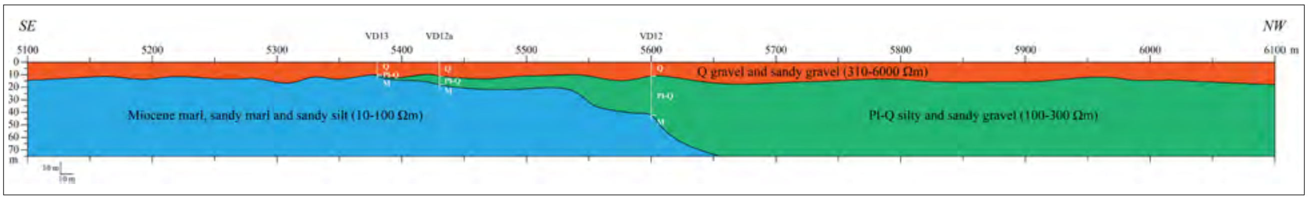

Fig. 12. Simplified geological cross section based on interpreted geoelectrical models and borehole data.
Sl. 12. Poenostavljen geološki prerez, izdelan na podlagi geoelektričnih raziskav in podatkov vrtin.

possible to successfully determine areas of three expected stratigraphic members and limit the electrical resistivity range for each. The highest values (310-6000 Ωm) represent Q gravel, which overlies the older sediments along the entire section to a depth of 10-15 m. A layer with very low electrical resistivities is deposited between profile station points of 5100 and 5400 m. It belongs to the response of Miocene (sandy) marl sediments. From 5400 m towards NW, presence of the medium resistive layer is evident, which we believe is a response of Pl-Q silty and sandy gravel. Its thickness increases gradually from 0 to over 50 m. Moreover, it is obvious that very low resistive Miocene sediments are deposited under the Pl-Q layer.

The boundary is well defined between Q and Pl-Q and also between Q and Miocene sediments with distinctive contrasts in electrical resistivity. The oblique boundary between Pl-Q and Miocene sediments was not defined so well, but with the use of different inversion parameters it was possible to determine its shape. However, as long as the Pl-Q layer is thinner than 3 m, its appearance is not evident on the geoelectrical models. This limitation cannot be surpassed with the existing modelling tools. After our analysis the extent of the Pl-Q layer is better visible on the models created with RES2DINV.

Parameters were evaluated based on the interpreted models. For our case the Occam's regularization method produced best models when used with lower vertical/horizontal flatness ratio. In the case of RES2DINV, better results were achieved with the use of different damping factors and combination of Occam's and ridge regression inversion methods.

As the final conclusion we propose a simplified geological cross section based on the interpreted geoelectrical models and borehole data (Fig. 12). From this cross section we are able to better determine suggested depth of the jet grouting sealing curtain along the investigated profile, which is certainly needed in the Q gravel and at least in upper parts of Pl-Q silty and sandy gravel. For the deeper parts of Pl-Q silty and sandy gravel, an additional evaluation is necessary to ponder on the construction costs and lateral outflow loss.

References - Literatura

Car, M. 1995: Geofizikalna tehnika zveznega električnega upornostnega sondiranja in njena uporaba v inženirski geologiji. Rudarsko-metalurški zbornik, 42/3–4: 109–126.

Car, M. & Stopar, R. 2008: Izvedba programa dopolnilnih začetnih terenskih raziskav geosfere in hidrosfere za potencialno lokacijo Vrbina v občini Krško ter za izvedbo programa začetnih terenskih raziskav geosfere in hidrosfere za potencialno lokacijo Vrbina, Gornji Lenart v občini Brežice, Vrbina, občina Krško: Segment 3: Površinske geofizikalne raziskave. Ljubljana: Geoinženiring d.o.o.

Fehdi, C., Baali, F., Boubaya, D. & Rouabhia, A. 2011: Detection of sinkholes using 2D electrical resistivity imaging in the Cheria Basin (north–east of Algeria). Arabian Journal of Geosciences, 4/1-2: 181–187, doi:10.1007/s12517-009-0117-2.

Lapajne, J. 1975: Geofizikalne raziskave vodonosnikov v Sloveniji. Geologija, 18: 339–355.

Loke, M. H. 2010: RES2DINV ver. 3.59 - Rapid 2-D Resistivity & IP inversion using the least-squares method [computer program and user's manual]. Penang, Malaysia: Geotomo Software.

Loke, M. H. 2014: Tutorial: 2-D and 3-D electrical imaging surveys. Penang, Malaysia: Geotomo Software (online). Internet: http://www.geotomosoft.com/coursenotes.zip.

Møller, I., Sørensen, K. I. & Auken, E. 2006: Geoelectrical methods. In: Kirsch, R., Rumpel, H.-M., Scheer, W., Wiederhold, H. (eds.): Groundwater Resources in Burried Valleys: A Challenge for Geosciences. BurVal Working Group 2004–2006. Hannover: Leibniz Institute for Applied Geosciences (GGA-Institut), 77–87.

Stoyer, C. & Butler, M. S. 2001: RESIX 2DI™ v4.14 – Resistivity Data Interpretation Software [computer program]. Golden Colorado, USA: Interprex Limited.

Van Overmeeren, R.A. & Ritsema, I. L. 1988: Continuous vertical electrical sounding. First Break, 6: 313-324.